

Material Damping Experiments at Cryogenic Temperatures

Marie Levine* and Christopher White
California Institute of Technology, Jet Propulsion Laboratory
4800 Oak Grove Dr., Pasadena CA 91109

ABSTRACT

A unique experimental facility has been designed to measure damping of materials at cryogenic temperatures. The test facility pays special attention to removing other sources of damping in the measurement by avoiding frictional interfaces, decoupling the test specimen from the support system, and by using a non-contacting measurement device. Damping data is obtained for materials (Al, GrEp, Be, Fused Quartz), strain amplitudes ($< 10^{-6}$ ppm), frequencies (20Hz-330Hz) and temperatures (20K-293K) relevant to future precision optical space missions. The test data shows a significant decrease in viscous damping at cryogenic temperatures and can be as low as $10^{-4}\%$, but the amount of the damping decrease is a function of frequency and material. Contrary to the other materials whose damping monotonically decreased with temperature, damping of Fused Quartz increased substantially at cryo, after reaching a minimum at around 150°K. The damping is also shown to be insensitive to strain for low strain levels. At room temperatures, the test data correlates well to the analytical predictions of the Zener damping model. Discrepancies at cryogenic temperatures between the model predictions and the test data are observed.

1. INTRODUCTION

As part of NASA's Origins Program, the James Web Space Telescope (JWST) is an orbiting observatory planned for launch circa 2010. Its mission, in part, is to observe cosmic objects associated with the origins and beginnings of the universe. These objects appear red-shifted in the current epoch, meaning we receive their radiation shifted towards the infrared region of the electro-magnetic spectrum. Reduction of thermal emissions of the telescope's primary and secondary mirrors and their supporting structures, by maintaining the entire structure below 50K, is essential to achieving the required signal-to-noise ratios for the observations. Very low levels of structural vibration are also required. Associated with small strains and extremely cold temperatures is the expected diminution of structural damping. Low structural damping increases optical alignment jitter due to higher amplitude vibration response to on-board dynamic disturbances and to increases in settling time after spacecraft slew maneuvers. The series of experiments reported in this paper were conducted to provide insight into the role temperature, frequency and strain play in influencing vibration damping in materials.

Vibration damping of built-up structures derives from contributions of material damping, friction at joints and interfaces, and discrete dampers or auxiliary vibration absorbers. Although rarely quantified, non-structural components such as multi-layer insulation and wiring harnesses may also contribute significant damping to lightly damped systems. However, these auxiliary damping mechanisms will only increase the amount of damping already provided by the material itself. Hence, this work is restricted to measuring damping for materials that are of immediate interest to JWST, and for which the experimental data will provide a lower bound damping estimate for the JWST analytical simulations. The materials tested include aluminum 6061-T6, several graphite/epoxy composites, optical-grade O-30H beryllium and fused quartz. A welded connection in aluminum and an adhesive splice joint in the graphite composite were also tested.

Material damping is a function not only of material, but also of temperature, frequency, configuration, strain sense, strain amplitude, and environmental effects. In the case of laminated composite materials, fiber volume ratio, lay-up orientation, and internal damage from past loading events also play a significant role. This complicates the comparison between different tests and makes it difficult to extrapolate to other situations. Of the measurements that have been reported in the literature, certain conclusions are relevant

to the present work. Room-temperature experiments have shown that for 2024-T3 and 6061-T6 aluminum alloy and graphite/epoxy composites in bending, damping is independent of strain and frequency as long as strain is below 10 microstrains. Above 100 microstrain, material damping increases with increasing strain [16]. Experiments with graphite/epoxy composites, also in bending, have shown that for the same number of laminae, changing the ply orientation from unidirectional $[0]_8$ to $[90]_8$ causes an order of magnitude increase in damping [18]. Tests with bars and tubes of aluminum in bending indicated that tubes have a factor of ten lower damping than bars. In contrast, both bars and tubes of graphite epoxy demonstrated nearly the same damping levels [16]. It is clear that in judging material damping, temperature and strain are but two variables in the trade space.

Relatively few cold-temperature measurements of material damping have appeared in the open literature. Katterloher [10] measured damping and frequency down to 4.5K for DISPAL2, MIC-6, and Al 6082 specimens, using a 170 Hz cantilevered beam configuration. Viscous damping values of the order of 10^{-5} at 77K were reported, with roughly a factor of 6 increase in damping at 293K. Zhang [12] tested a 130 Hz cantilever specimen of aluminum alloy at 4.2K, and reported a viscous damping value of 0.004, but concluded that the damping measurements were influenced by the presence of nitrogen or helium gas in the Dewar. Aaron [13] measured frequency and damping of a Teflon cantilever beam and reported values of 12.5 Hz and 0.0013 at 77K, and 5.4Hz and .04 at 293K. Okada et. al. [11] suggested using Young's modulus and damping as indicators of fatigue damage in glass-reinforced epoxy composites. Their measurements showed strong unimodal temperature dependence for damping, with maximum damping of 0.015 occurring at 250K.

For b.c.c. and f.c.c. cubic lattice structured metals, Zener theory predicts the thermo-elastic energy loss in beams undergoing cyclic bending strains. Dependence on temperature, frequency, and beam thickness are captured in the theory; however, the theory does not apply for axial and torsional strains, for materials other than b.c.c. and f.c.c metals, or for configurations other than rectangular beams. Many room temperature damping measurements have been made to validate the Zener theory, with much success [15-18]. Predictive models for material damping in fiber-reinforced composites have been proposed. A detailed summary of the available models is provided in [14].

To provide insight into material damping levels at cryogenic temperatures, the present experiments were designed such that a beam-like specimen of material was supported as a pendulum from very thin suspension wires, brought to near 30K inside a thermal vacuum chamber, then quickly struck by an impact force; the ensuing vibration decay was measured by a non-contacting laser, from which viscous damping ratios were determined.

2. EXPERIMENTAL SETUP

All measurements were made in the Cryocooler Characterization Lab at the Jet Propulsion Laboratory. The tests were performed inside a 0.6m diameter thermal vacuum chamber equipped with a Gifford-McMahon cycle cryocooler. The system is capable of maintaining the cold finger at any arbitrary temperature between 293K and 11K, but for various practical reasons the minimum specimen temperature was 21K. Pressure inside the chamber was maintained between 10^{-5} to 10^{-6} Pa.

An aluminum framing fixture within the chamber supported the specimen as a pendulum and served as a mounting platform for accessories such as cameras and mechanical linkages which control the height of the specimen.

The specimens were prismatic rectangular beams with length 508mm, height 50.8mm, and thickness that varied among specimens. Two stainless steel suspension wires of 0.281mm diameter and 838mm length were attached to the top edge of the specimen at the two nodal points of the first transverse bending mode. This support configuration minimizes interaction between the specimen bending mode and the modes of the suspension system. In the initial configuration, a 20mm diameter solenoid actuator controlled by a quick-discharge capacitor was used to quickly strike the specimen. For later tests, the solenoid striker was replaced with a curved tube which guided a 6 mm diameter steel or plastic ball through free-fall to collide

with the specimen in a horizontal direction. This enhancement enabled a repeatable impact force to strike the specimen, the magnitude of which was determined by the mass of the ball.

A copper box-shaped dewar enclosed the specimen to shield it from radiation heating. The dewar had openings on three sides: two slots on the top for the specimen suspension wires, a 10mm hole on one side for the laser beam, and a 15mm hole on the opposite side for the solenoid shaft or curved tube.

Transverse velocities of the vibrating specimen were measured using a non-contacting laser vibrometer which shone through a $\frac{1}{10}$ optical quality viewport. To enhance the optical diffusivity of the specimens, a 25mm square piece of retro-reflective tape was attached as a target for the laser beam. Both the impact force and the laser measurements occurred at the geometrical center of the specimen. An 8mm diameter, 1g, brass temperature diode was epoxied to the specimen just underneath one of the suspension wires. The 0.30mm lead wire was carefully run up the suspension wire, being careful to keep sufficient slack in the lead to minimize interaction. Three additional temperature sensors monitored critical locations within the chamber. The original set-up also included a high sensitivity piezoelectric strain gauge and a cryogenic accelerometer as witness sensors for measurement verification. However, they were removed as the small wires connecting the sensors were found to increase the damping estimate by at least factor of 2.

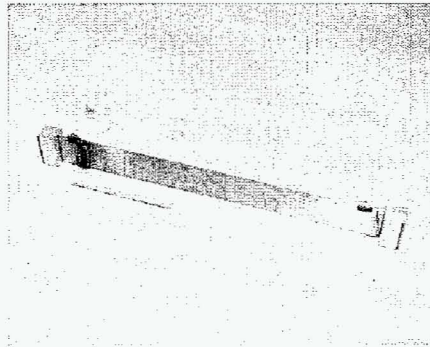


Figure 1 Close-up of specimen showing support points and end masses

3. THEORETICAL BACKGROUND

The Zener theory relates damping to temperature, material properties, thickness, and vibration frequency as follows:

$$\xi = \frac{\alpha^2 ET}{2C_p \rho} \left[\frac{\omega \tau}{1 + (\omega \tau)^2} \right] \dots 1 \quad \tau = \frac{C_p h^2 \rho}{\kappa \pi^2} \dots 2$$

in which α is coefficient of thermal expansion (1/K), h is specimen thickness (m), E is elastic modulus (N/m²), T is temperature (K), C_p is specific heat (J/kg/K), κ is thermal conductivity (W/m/K), ρ is density (kg/m³), ω is frequency of vibration (rad/s), π is 3.14159, and τ is relaxation time (s/rad). It is frequently more convenient to work with the relaxation frequency (1/ τ) instead.

4. DATA ANALYSIS

Absolute velocity of the swinging and vibrating specimen was measured with the laser vibrometer and sampled and digitized with a 16 bit data acquisition system. Depending on the specimen and the expected damping, record lengths of up to 60 seconds at a rate of between 5120 samples/s to 10240 samples/s were recorded. A fourth-order Butterworth digital band-pass filter was applied in the forward and backward directions around the fundamental bending frequency to remove all other modes of vibration and the swinging and twisting pendulum motions. Measured velocities were then converted to extreme fiber strains using the analytical solution for the fundamental mode shape of a free-free beam, in conjunction with the strain-displacement relationship for Euler-Bernoulli beam theory. The result is dependent only on frequency of vibration and beam thickness (both of which are measured directly), not on material properties. After filtering, the record was searched sequentially and the sample with the maximal positive value in each cycle of vibration was selected and retained, to form an envelope of decaying peak amplitudes.

Working with 250 peak values at a time, a least-squares regression analysis was used to compute the best viscous damping coefficient for that window of data. The 250-sample window was then advanced one peak forward in time and the regression analysis was repeated, continuing until the entire record length had been analyzed and an estimate of viscous damping versus time (or peak amplitude) had been formed. For most records, it was then necessary to average this result across the entire time record because the damping estimate oscillated with the swinging of the specimen in the pendulum mode. Damping estimates measured from separate tests using a strain gage did not exhibit the oscillations and thus it was concluded that the oscillations are related to the laser measurement. One possible explanation is that the laser beam is not measuring the same location at every instant, but is instead roving over a very small area of the specimen due to bar displacement related to swinging.

5. ERROR SOURCES

As part of the experimental procedure, each test was repeated 3 times, and the reported damping estimate is the average of the 3 results. The standard deviations were typically 1% to 10% of the damping value depending on amplitude, and the accuracy was observed to be approximately 2e-6. In some instances the samples were subjected to multiple thermal cycles and the damping estimates were repeatable to several percent.

The potentially largest errors in the damping estimates come from pendulum motions (two modes of swinging, and one mode of twisting), from higher-mode effects, from parasitic losses due to lead wires, and from discretization and quantization. Interaction with the pendulum modes would tend to increase the damping measurements and was minimized or eliminated by keeping the pendulum modes low in frequency and well-separated from the vibration modes, and by filtering the raw measurements as described above. Impact forces excite many modes other than the fundamental bending mode of the specimen. This has consequences when the damping is strain-dependent, as the decomposition of

vibrations into orthogonal modes is no longer applicable. Parasitic losses also increase damping measurements and were eliminated by using only non-contacting measurement techniques. As discovered early in the test program, even the micro-dot cables for tiny strain gauges caused the lowest measured damping levels ($\sim 5 \cdot 10^{-6}$) to double and become unrepeatable from test to test. Discretization errors in the digital processing of the sensor signals can be significant at very low damping levels if the discretization introduces systematic errors by not sampling at the peak amplitude for each cycle. These seemingly small errors in amplitude can easily ruin very small damping measurements. Quantization errors are minimized by use of a 16 bit system and by properly adjusting the full scale range.

6. RESULTS

6.1. ALUMINUM 6061-T6

Table 1 summarizes the five samples of aluminum 6061-T6 tested. The last column in Table 1 shows the mass attached to each end of the specimen to lower the vibrational frequency. At each end, the lumped mass consists of two blocks, each measuring 50.8x25.4x13mm, attached with epoxy adhesive to both faces of the bar. The welded specimen was fabricated by cutting a continuous bar into two sections that were then double-groove welded back together at a point one-third the way along the length of the bar. The weld conforms to AMS-STD-2219.

Table 1 Physical Dimensions of 6061-T6 Aluminum Samples

Specimen	Thickness (mm)	Nominal Frequency at 293K (Hz)	Support Separation (mm)	End Mass (kg)
Al-A	6.267	126	279	0
Al-B	3.142	63	279	0
Al-C	1.510	31.5	279	0
Al-D	1.510	18.2	406	0.1880
Al-Weld	6.291	126	279	0

Viscous damping values versus temperature are shown in Figure 2 for specimens Al-A, -B, -C, and -D. The measurements at 293K have been compared to the Zener theory in Figure 3 by plotting measured and predicted damping as a function of the frequency of free vibration normalized by the relaxation frequency. One sees that the Zener theory underestimates damping at higher frequencies, a trend which has also been reported by other studies [15,17].

A similar comparison to Zener theory is made in Figure 4 for the measurements at 40K. While the measurements and the theory do not agree at cold temperatures, Zener theory is not necessarily invalidated at cold temperatures, as the prediction is based on cold-temperature material properties taken from a handbook and which may vary considerably from the actual properties of the vibration samples. Nevertheless, the close agreement at 293K serves to validate the experimental approach and data analysis techniques.

A sample of filtered data from specimen Al-B at 293K is shown in Figure 5. The lower subplot shows the peak positive values for each cycle of oscillation that are subsequently used in the least-squares regression calculations. The degree to which the data fits the amplitude-independent viscous damping assumption is seen in Figure 6, where the logarithm of the peaks in Figure 5 has been plotted against time. Note how the slope oscillates as a result of the swinging motion, and how the data gets "noisy" at small strain levels as the signal-to-noise ratio decreases. Figure 6 is representative of all measurements made on Al 6061-T6 and it is concluded that for practical purposes the damping was independent of strain.

The comparison between the continuous and the welded aluminum samples is shown in Figure 7. Finally, the temperature dependence is summarized in

Table 2, where the ratio between the room temperature damping and damping at 40K is shown.

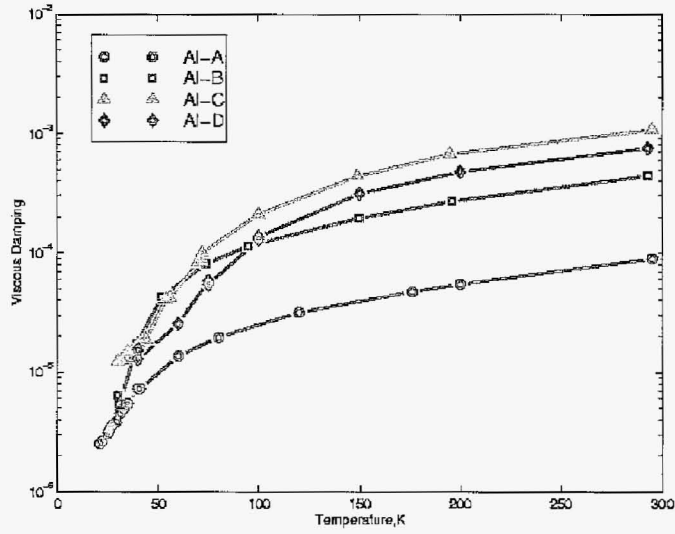


Figure 2 Measurements for 6061-T6 aluminum samples.

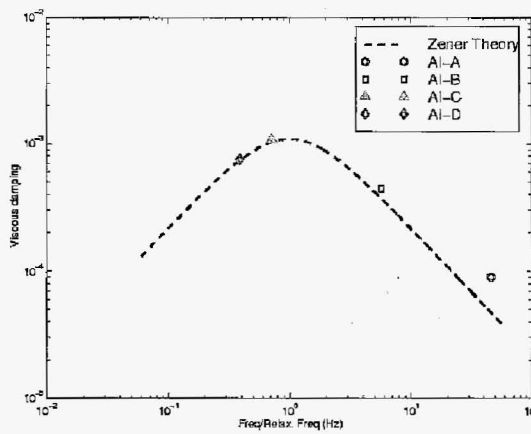


Figure 3 Comparison to Zener Theory at 293K.

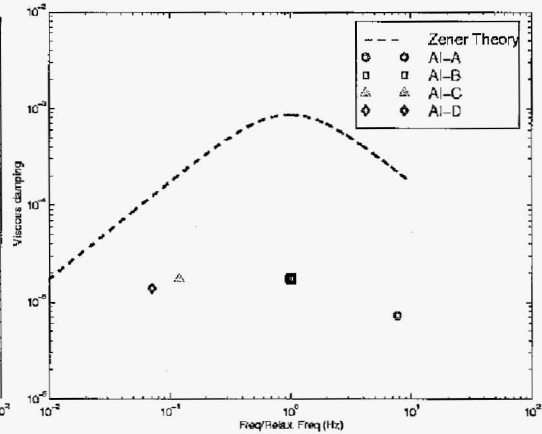


Figure 4 Comparison to Zener Theory at 40K.

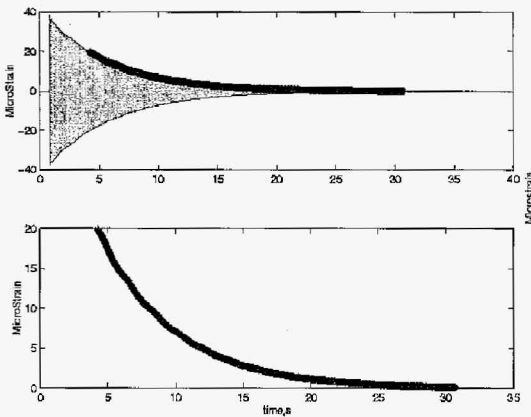


Figure 5 Free decay of Specimen Al-B at 293K.

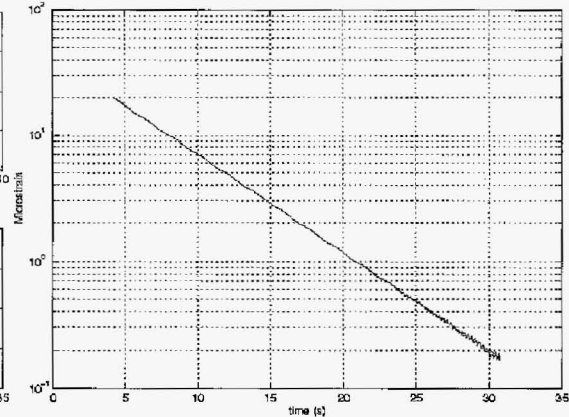


Figure 6 Logarithm of free decay amplitudes plots as a straight line when damping is viscous.

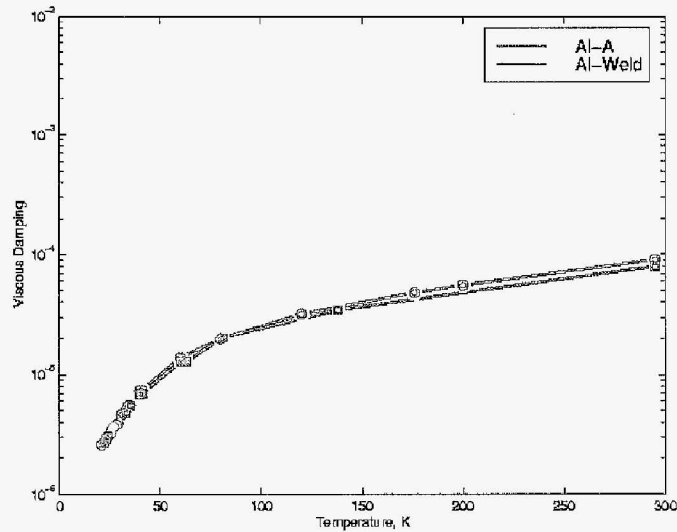


Figure 7 Little difference in damping was measured between the continuous and the welded Al beam.

Table 2 Summary of measured damping values for 6061-T6 Aluminum

Sample	ζ_{293}	ζ_{40}	Ratio ζ_{293}/ζ_{40}
Al-A	9.0e-5	0.74e-5	12.2
Al-B	44.8e-5	1.8e-5	24.9
Al-C	109e-5	1.8e-5	60.6
Al-D	75.5e-5	1.4e-5	53.9
Al-Weld	8.1e-5	0.69e-5	11.7

6.2. GRAPHITE-EPOXY COMPOSITES

Data for the graphite-epoxy composite specimens are listed in Table 3. Specimens GrEp-A, -B, and -C are continuous bars, each of a different material, while Specimen GrEp-D is constructed of two half-sections butt-jointed at the centerline, then reinforced with splice plates on both faces. The splice plates have a total length of 202 mm, and are attached symmetrically about the centerline with EA9394 adhesive. While it is known that each bar is a different composite material, the fiber lay-up and other specifics are considered proprietary information, and are not known to the authors.

Damping values measured in the present tests are presented graphically in Figure 8. The present measurements (at room temperature) compare closely with those of Ting and Crawley [16] who measured damping ratios between 2.56e-04 and 3.35e-04 for $[0]_{24}$ GrEp bars, and damping values between 6.24e-04 and 11.1e-04 for $[15]_{6s}$ GrEp bars. The present data shows no obvious trends with frequency or thickness, although the sample with the splice plate does have the largest damping. Table 4 summarizes the damping at room temperature and at 40K. It is evident that damping of the GrEp samples is less sensitive to temperatures than the damping of the aluminum samples.

As with the aluminum samples, for engineering purposes, damping was found to fit a viscous damping model, independent of strain, within the range of approximately hundreds of nanostrain to a few microstrain, as shown in Figure 9. This conclusion is also largely supported by the data of Ting and Crawley [16].

Table 3 Dimensions of the Graphite-Epoxy Samples

Specimen	Thickness (mm)	Nominal Frequency at 293K (Hz)	Support Separation (mm)
GrEp-A	2.81	140	279
GrEp-B	1.49	48	279
GrEp-C	2.16	97	279
GrEp-D	2.16 / 7.24 / 2.16	134	406

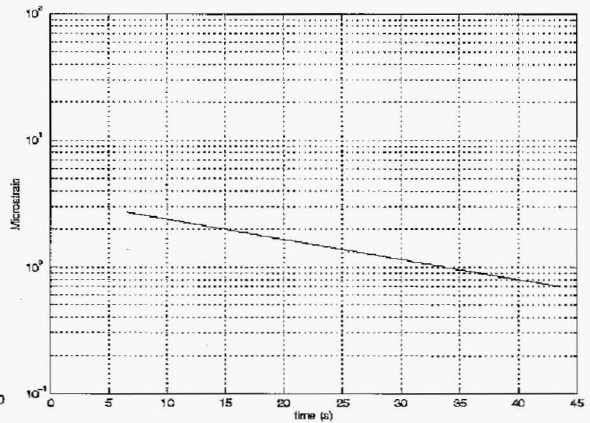
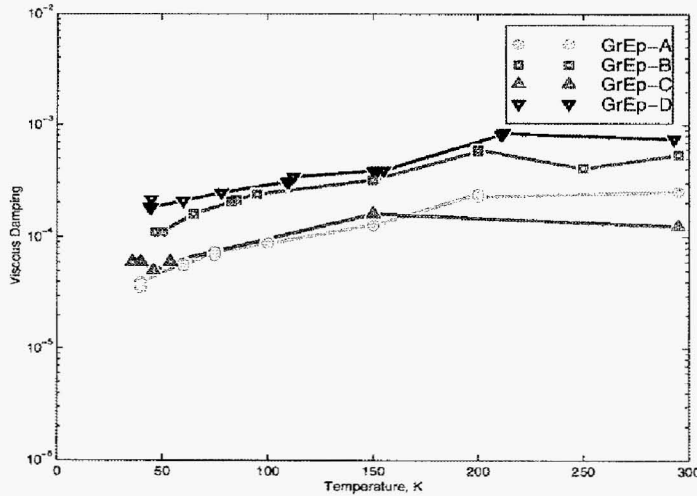


Figure 8 Damping measurements for the four GrEp specimens.

Figure 9 Free decay amplitudes for specimen GrEp-C at 40K.

Table 4 Summary of measured damping values for GrEp.

Sample	ζ_{293}	ζ_{40}	Ratio ζ_{293}/ζ_{40}
GrEp-A	25e-5	3.6e-5	6.9
GrEp-B	54e-5	10e-5 (est.)	5.4
GrEp-C	13e-5	5.5e-5	2
GrEp-D	75e-5	18e-5	4.2

6.3. BERYLLIUM

Samples of O-30H beryllium measuring 50.8 mm by 508 mm and of various thicknesses were tested. Table 5 summarizes the key dimensions. The end blocks measure 50.8x24.8x 12.4mm each, and were glued onto both faces of the bar for sample Be-D.

The damping ratios measured on these samples are shown in, and compared in Table 6. In comparison to the aluminum and GrEp samples, the data reveals a large variation in room-temperature damping among the four samples. This is a result of including sample Be-A with a very high natural frequency of 337 Hz. In examining, it is interesting to note that the damping of these samples is rather insensitive to decreasing temperatures until somewhere near 60K, at which point the damping falls off sharply. The reason for this behavior is not understood at this time.

A comparison between the beryllium measurements and the Zener theory damping predictions is made in Figure 11 and Figure 12. Again, the room temperature measurements, or at least their trends, are in close agreement with the

theory, while the measurements at 40K are two to four orders of magnitude larger than the predictions. It should be mentioned again that the predictions at 40K are based on material properties that were taken from the technical literature and may not accurately represent the cold-temperature properties of the samples used in the vibration testing.

Table 5 Physical dimensions of Beryllium samples

Specimen	Thickness (mm)	Nominal Frequency at 293K (Hz)	Support Separation (mm)	End Mass (kg)
Be-A	6.50	337.2	279	0
Be-B	2.65	137.1	279	0
Be-C	1.40	72.5	279	0
Be-D	1.40	40.8	418	0.064

Table 6 Summary of measured damping values for Beryllium

Sample	ζ_{293}	ζ_{40}	Ratio ζ_{293}/ζ_{40}
Be-A	3.8e-5	2e-5	1.9
Be-B	28e-5	4e-5	7
Be-C	88e-5	8e-5	11
Be-D	91e-5	8e-5	11.4

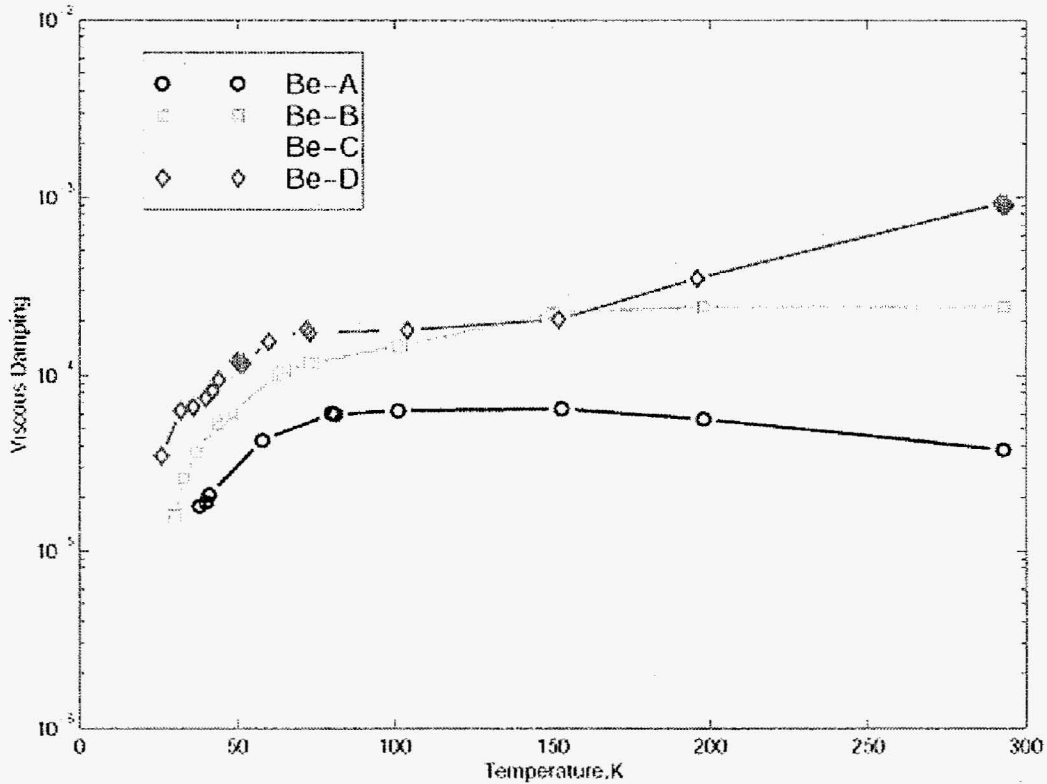


Figure 10 Damping measurements for the O-30H Beryllium samples

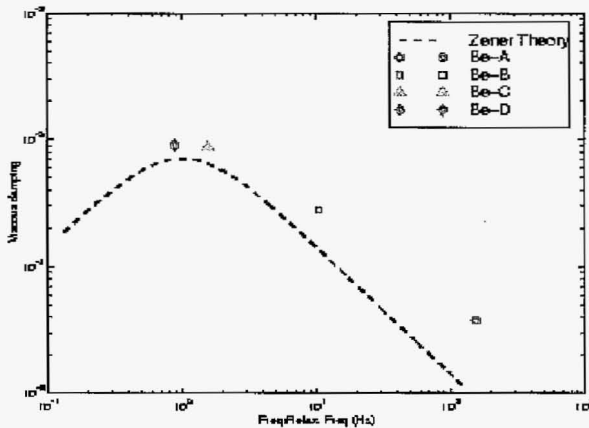


Figure 11 Comparison to Zener theory at 293K

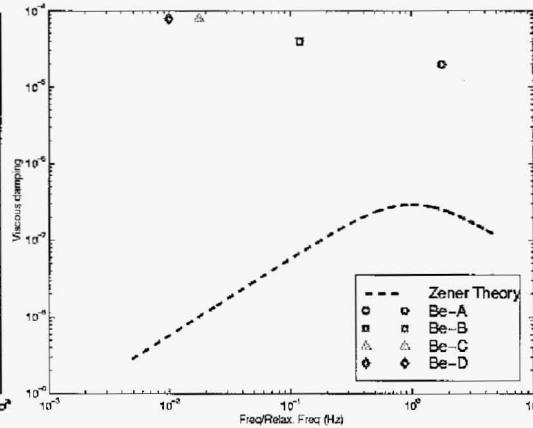


Figure 12 Comparison of Be O-30H measurements to Zener Theory at 40K

6.4. FUSED QUARTZ

Vitreasil Clear Fused Quartz (CFQ) from Saint-Gobain Quartz was tested for its damping properties. Quartz is known for its low damping properties and provides a good benchmark test case for the accuracy of the measurement system. Although this particular material is not optical grade, the overall damping trend should not be affected. Nonetheless, higher grade material contains less bubble concentration and has a slightly different chemical composition. Since material structure and composition affects damping, subsequent testing of optical grade glass relevant to the JWST mission is highly recommended.

For the current experiments only 2 thicknesses of fused quartz were tested for fear that thinner samples would crack from the ball impact. Fortunately, no visible cracks developed in the samples during testing. The sample dimensions and associated frequencies are summarized in Table 7. Contrary to the previous materials tested, the modal frequencies decrease as a function of temperature and by approximately 1.7%. Equivalently the material stiffness decreases by about 3%. This softening behavior at cryo is consistent with elastic modulus properties reported in the literature.

Table 7 Dimensions of the Fused Quartz Samples

Specimen	Thickness (mm)	Nominal Frequency at 293K (Hz)	Nominal Frequency at 30K (Hz)	Support Separation (mm)
FQ-A	6.35	147	144.5	279
FQ-B	3.175	71.2	69.8	279

The measured damping as a function of temperature and frequency are presented in Figure 13 and compared in Table 8. Again, contrary to the materials tested beforehand, damping of quartz increases by a factor of 30 at cryo relative to room temperature, and this increase is not monotonic with temperature. Quartz damping reaches a minimum between 100K and 175K, depending on frequency, and is measured to be as low as 1e-6. However, this is also the limit of accuracy of the damping measurement technique, so the actual damping may be even lower.

The quartz's damping trend is not completely unexpected since according to the Zener theory (Eq. 1) damping is proportional to the elastic modulus and to the square of the CTE. For quartz both these properties increase at cryogenic temperatures, and CTE reaches a minimum around 50K to 70K. However, correlation to the Zener damping prediction was unsuccessful here because the relaxation frequencies were 2 to 3 orders of magnitude smaller than the tested modal

frequencies and because Zener theory specifically applies to metals. Hence, further testing is recommended to determine if this damping behavior also applies to glass materials, grades, thicknesses and frequencies relevant to the JWST design.

Table 8 Summary of measured damping values for Fused Quartz

Sample	ζ_{293}	ζ_{40}	Ratio ζ_{293}/ζ_{40}
FQ- A	1.44 e^{-5}	3.75 e^{-4}	0.038
FQ -B	1.02e^{-5}	3.15 e^{-4}	0.032

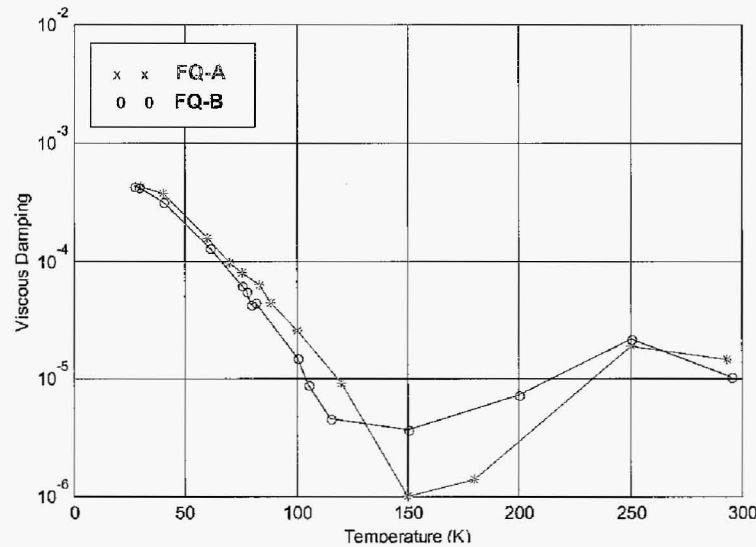


Figure 13 Damping measurements for the Fused Quartz samples.

7. CONCLUSIONS

The following conclusions are supported by the measurements:

1. Except for fused quartz, the measurements establish the general trend of decreasing damping with decreasing temperature. For the majority of the samples, this trend is monotonic, although several samples of graphite-epoxy and beryllium had a peak value at a lower temperature that was slightly higher than the room temperature value, but this increase was small compared to the overall loss in damping that takes place when temperature is decreased to 40K.
2. Except for fused quartz, no lower bound on material damping was observed in the measurements. Additionally, each sample shows a different rate of damping decrease with temperature in the vicinity of 40K.
3. Fused quartz damping behavior as a function of temperature is substantially different than for the other materials tested herein: damping increases at cryogenic temperature, is not monotonic and reaches a minimum of 1e^{-6} or less at approximately 150K. As predicted by the Zener damping theory, this behavior could be linked to the material's trends in CTE and modulus of elasticity at cryogenic temperatures. Additional damping tests are recommended on grades of glass intended for JWST.
4. A viscous, strain-independent damping model at all temperatures is a reasonable engineering approximation for the range of strains examined in these experiments.

5. The applicability of the Zener damping theory is confirmed for aluminum and beryllium at room temperature. At 40K the theory has not been confirmed. Based on handbook values for thermo-mechanical material properties, the measurements and the predictions are in error by up to four orders of magnitude. No independent measurements of material properties for the actual aluminum and beryllium samples tested for damping have been made, so the possibility remains that the Zener theory is valid at 40K when the correct material properties are introduced.
6. Using the ratio of ζ_{293}/ζ_{40} as a metric for comparing the change in damping with temperature, aluminum is the most sensitive with ratios between 12 and 61 (depending on the sample), beryllium was the next most sensitive with ratios between 2 and 12, and the graphite epoxy samples were the least sensitive, with ratios between 2 and 7. For fused quartz the ratios were approximately 0.02.
7. The presence of a weld has no appreciable effect on damping at any temperature. The graphite-epoxy sample with butt joint and splice plates had a larger damping ratio than the continuous graphite-epoxy samples.

These material damping measurements and the conclusions described above are valid for rectangular bars subjected to bending strains only. Different damping values may be measured for axial strains, for torsional strains, for different cross sections, for different bending frequencies, etc. Built-up structures, particularly where they include joints or connections or other elements typically assumed to contribute little damping, may actually have inherent damping many times larger than the values reported here. It is recommended to follow this material damping study with tests of built-up components.

8. ACKNOWLEDGEMENTS

This work was performed at the Jet Propulsion Laboratory, California Institute of Technology, under contract with the National Aeronautics and Space Administration.

9. REFERENCES

10. Katterloher, R.O., "Low Temperature Decay of Vibrational Resonance for Bars Made of DISPAL2 Sintered Al-Powder, Alloy MIC-6, and AlMgSil," *Proceedings of the Twelfth International Cryogenic Engineering Conference, ICEC 12*, Southampton, UK, 1988. pp. 455-9.
11. Okada, T., S. Nishijima, K. Matsushita, T. Okamoto, H. Yamoka, and K. Miyata, "Dynamic Young's Modulus and Internal Friction in a Composite Material at Low Temperatures," *Advances in Cryogenic Engineering Materials*, Vol. 30, 1984.
12. Zhang, Z., L.Z. Zhao, Z.H.Tu, P.Q.Zhang, "Dynamic Young's Moduli of Space Materials at Low Temperatures," *Cryogenics*, Vol. 34 No. 10, 1994.
13. Aaron, K., "Low Amplitude Material Damping Measurements at 77 Kelvin", personal communication. 1997.
14. Chandra, R., S. P. Singh, K. Gupta, "Damping Studies in Fiber-Reinforced Composites – A Review," *Composite Structures*, Vol. 46, 1999.
15. Crawley, E.F., M.C. Van Schoor, "Material Damping in Aluminum and Metal Matrix Composites," *Journal of Composite Materials*, Vol. 21, Jun. 1987.
16. Ting, J., E.F. Crawley, "Characterization of Damping of Materials and Structures at Nanostrain Levels," M.S. Thesis, M.I.T., June 1990.
17. Crawley, E.F., R.L. Sheen, "Experimental Measurement of Material Damping for Space Structures," Proc. Of Vibration Damping Workshop, Long Beach, CA, Feb. 1983.
18. Crawley, E.F., G. L. Sarver, and D.G. Moore, "Experimental Measurement of Passive Material and Structural Damping for Flexible Space Structures," *Acta Astronautica*, Vol. 10, No. 5-6, 1983.
19. Zener, C., *Elasticity and Anelasticity of Metals*, University of Chicago Press, 1948.
20. *Cryocomp Computer Program*, Version 3.05, Eckels Engineering, Inc., Florence, SC.
21. Paquin, R. Professional correspondence addressed to T. Parsonage, dated January 27, 1984.
22. Barron, T.H.K, and G.K. White, *Heat Capacity and Thermal Expansion at Low Temperatures*, Plenum Pub Corp, June 1999.